


Aberrant insular cortex connectivity in abstinent alcohol-dependent rats is reversed by dopamine D3 receptor blockade

Giulia Scuppa¹  | Stefano Tambalo¹ | Simone Pfarr² | Wolfgang H. Sommer^{2,3} | Angelo Bifone^{1,4}

¹Center for Neuroscience and Cognitive Systems, Istituto Italiano di Tecnologia, Rovereto, Italy

²Institute of Psychopharmacology, Central Institute of Mental Health, University of Heidelberg, Mannheim, Germany

³Department of Addictive Behavior and Addiction Medicine, Central Institute of Mental Health, University of Heidelberg, Mannheim, Germany

⁴Department of Molecular Biotechnology and Health Sciences, University of Torino, Torino, Italy

Correspondence

Giulia Scuppa and Angelo Bifone, Center for Neuroscience and Cognitive Systems, Istituto Italiano di Tecnologia, Corso Bettini, 31 I-38068 Rovereto, Italy.
Email: giulia.scuppa@iit.it; angelo.bifone@iit.it

Funding information

European Union's Horizon 2020, Grant/Award Number: 668863

Abstract

A few studies have reported aberrant functional connectivity in alcoholic patients, but the specific neural circuits involved remain unknown. Moreover, it is unclear whether these alterations can be reversed upon treatment. Here, we used functional MRI to study resting state connectivity in rats following chronic intermittent exposure to ethanol. Further, we evaluated the effects of SB-277011-a, a selective dopamine D3 receptor antagonist, known to decrease ethanol consumption. Alcohol-dependent and control rats ($N = 13/14$ per group), 3 weeks into abstinence, were administered SB-277011-a or vehicle before fMRI sessions. Resting state connectivity networks were extracted by independent component analysis. A dual-regression analysis was performed using independent component maps as spatial regressors, and the effects of alcohol history and treatment on connectivity were assessed. A history of alcohol dependence caused widespread reduction of the internal coherence of components. Weaker correlation was also found between the insula cortex (IC) and cingulate cortices, key constituents of the salience network. Similarly, reduced connectivity was observed between a component comprising the anterior insular cortex, together with the caudate putamen (CPu-AntIns), and the posterior part of the IC. On the other hand, postdependent rats showed strengthened connectivity between salience and reward networks. In particular, higher connectivity was observed between insula and nucleus accumbens, between the ventral tegmental area and the cingulate cortex and between the VTA and CPu-AntIns. Interestingly, aberrant connectivity in postdependent rats was partially restored by acute administration of SB-277011-a, which, conversely, had no significant effects in naïve rats.

KEYWORDS

alcohol, D3 antagonist, fMRI, functional connectivity, insular cortex, postdependent rat

1 | INTRODUCTION

Alcohol use disorder (AUD) is an important public health issue with largely unmet medical needs. Several therapeutic strategies have been

investigated to control alcohol drinking, craving, and relapse in abusers. However, only a minority of the patients benefits from pharmacological treatments, and the relapse rate is still high. For this reason, understanding the neural mechanisms underlying alcohol

This is an open access article under the terms of the Creative Commons Attribution-NonCommercial-NoDerivs License, which permits use and distribution in any medium, provided the original work is properly cited, the use is non-commercial and no modifications or adaptations are made.

© 2019 The Authors. *Addiction Biology* published by John Wiley & Sons Ltd on behalf of Society for the Study of Addiction

addiction is of critical importance to identify molecular targets for the development of novel therapeutic approaches.

Functional magnetic resonance imaging (fMRI) enables the exploration of large-scale brain networks *in vivo*, non-invasively, and with high spatial resolution. Particularly, resting-state functional connectivity (rsFC) refers to fMRI data acquired in the absence of an explicit task and is assessed by measuring correlations of spontaneous fluctuations of blood oxygen level-dependent (BOLD) signals in different regions of the brain at rest.^{1,2} This technique has been widely applied to investigate the effects of various drugs and neuropsychiatric disorders on resting-state functional networks in both humans and laboratory animals, thus bridging clinical and preclinical research.^{3,4}

A few studies suggest that during abstinence AUD patients show aberrant patterns of resting state connectivity, with some inconsistent results. Indeed, several studies reported increased connectivity within prefrontal and frontobasal networks including default, salience, and executive networks in patients compared with controls.^{5,6} Others found weaker intrinsic connectivity in these networks.⁷ These discrepancies may result from the heterogeneity in patient populations such as duration and severity of AUD, duration of abstinence, comorbidity with other psychiatric disorders, concurrent consumption of other drugs of abuse, and effects of pharmacological treatments. All these factors could greatly impact brain functional connectivity and may bias inference regarding the effects of alcohol exposure.

Animal models of AUD can overcome some of these limitations as they allow *in vivo* manipulation of experimental factors within a well-controlled environment in a longitudinal perspective. Two essential conditions are required to develop AUD in humans—sufficiently high alcohol levels and exposure over long periods of time. To capture such conditions in rodents that do not voluntarily intoxicate themselves over prolonged periods of time, controlled forced administration paradigms are used. Chronic intermittent exposure (CIE) to daily cycles of alcohol intoxication and withdrawal over weeks or months mimics a pattern of alcohol use typically seen in clinical populations. Similar to AUD patients, animals show behavioral and neuroadaptive consequences that are induced as a subject becomes dependent on alcohol and remain for extended periods of time even in the absence of alcohol exposure—a condition referred to as a “postdependent state” (PD) and conceptualized as a model for the increased propensity to relapse in abstinent alcoholic patients.^{8,9} While this condition may not be considered as an addiction *per se*, PD rats show “addiction-prone” behavioral responses related to the motivational,¹⁰ emotional,¹¹ and inhibitory control circuits¹² comprising the tripartite addiction circuitry. Hence, the CIE procedure has become the dominant paradigm in preclinical AUD research and medication development of the last 15 years.^{9,13}

Here, we took advantage of the PD rat model to investigate whether a history of alcohol dependence has long-term effects on functional connectivity networks in the rat brain. To our knowledge, only one study investigated the effects of alcohol on brain connectivity in rodents via resting-state fMRI, focusing on the effects of binge-like adolescent alcohol exposure.¹⁴ In that study, several regions of interest were defined anatomically with the aim of elucidating frontostriatal alterations due to alcohol exposure. However the analysis did not take into account areas

such as the insular cortex (IC), which has been shown to be involved in alcoholism.^{15,16} The insula is central to the salience network, a key circuit involved in detection and processing of externally and internally generated salient stimuli.^{17,18} To overcome the need of a priori defined regions of interest, in the current work, we used a data-driven approach (decomposition by independent component analysis) to parcellate the brain into functional components. In addition, we aimed to test whether alcohol-induced alterations in functional connectivity may be reversed by pharmacological treatment. A powerful tool to specifically interfere with distinct network nodes within the reward system is provided by the D3 antagonist SB-277011-a, because its target dopamine D3 receptors are highly selectively expressed in the ventral striatum.^{19,20} Importantly, SB-277011-a has been previously shown to reduce seeking and taking of alcohol and other drugs of abuse in the rat.^{21–24} Hence, we here studied the ability of SB-277011-a to modulate the reward system and subsequent effects on overall network function in PD and nondependent (ND) rats.

2 | MATERIALS AND METHODS

2.1 | Animals

Male Wistar rats, initial weight 220 to 250 g, were used (Charles River), housed two to four per cage (Type-IV; Ehret) under a 12 hours light/dark cycle with *ad libitum* access to food and water. All experiments were conducted in accordance with the ethical guidelines for the care and use of laboratory animals and were approved by the local animal care committee (Regierungspräsidium Karlsruhe, Germany, license numbers: 35-9185.81/G-10/16 and Italian Ministry of Health, approval number: 796/2016-PR).

2.2 | Ethanol exposure

To induce dependence, rats were exposed to daily intermittent exposure cycles to alcohol vapour intoxication and withdrawal, a paradigm that allows a high degree of control over brain alcohol levels and induces behavioral and molecular changes relevant for the pathophysiology of alcoholism.^{9,25} Rats were weight-matched, assigned into the two experimental groups, and exposed to either ethanol vapour ($N = 13$, becoming PD) or normal air ($N = 14$, ND) using a rodent alcohol inhalation system as described previously.²⁶ Briefly, dosing pumps (Knauer) deliver alcohol into electrically heated stainless-steel coils (60°C) connected to an airflow of 18 L/min into glass and steel chambers (1 × 1 × 1 m). For the next 8 weeks, rats were exposed to five cycles of 14 hours of ethanol vapour per week (0:00 AM to 2:00 PM) separated by daily 10-hour periods of withdrawal. Twice per week, blood (~20 µL) was sampled from the lateral tail vein, and blood alcohol concentrations were determined using an AM1 Analox system (Analox Instruments). Blood alcohol level was monitored throughout the ethanol vapour exposure and the concentration maintained around 250 mg/dL (see SI, Figure S1). After the last exposure cycle, rats remained abstinent for 3 weeks before initiating the MRI scan.

2.3 | Drugs

SB-277011-a dihydrochloride (Tocris Bioscience) was dissolved in 20% w/v 2-hydroxypropyl-beta-cyclodextrin in water and administered according to a within-subject design, in a counterbalanced order, intraperitoneally, at a dose of 20 mg/kg/mL,^{27,28} 30 minutes before the beginning of the scan session.²⁹ Seven days of recovery were allowed between the two imaging sessions (see SI, Figure S2).

2.4 | Animal preparation for fMRI

For the rs-fMRI experiment, animals were initially anesthetized with 3% isoflurane in O₂:N₂O (3:7), which was then reduced to 1.5% for maintenance during preparation.³⁰ Subsequently, a bolus of 0.05 mg/kg/mL of medetomidine (Domitor, 1 mg/mL, Orion Pharma) was injected intraperitoneally, followed, 15 minutes later, by a continuous infusion of medetomidine diluted 1:5 in saline at a rate of 1 mL/kg/h through a catheter inserted subcutaneously.^{31,32}

After that, rats were injected with vehicle or SB-277011-a and then placed in the scanner. At this point, isoflurane was discontinued.

Scout images, shimming procedures, and structural scan were conducted in this time frame, while the functional imaging session started 30 minutes after the administration of the drug and at least 15 minutes after removal of isoflurane.

During the scan, respiration rate, heart rate, and blood oxygen saturation were monitored with a pulse oximeter (STARR Life Science, USA). CO₂ concentration in the blood was also assessed using a TCM4 Transcutaneous Blood Gas Analyzer (Radiometer Copenhagen). Rectal temperature was maintained at 37°C during the experiments by a feedback-controlled, water-circulating heating pad. At the end of the fMRI experiment, medetomidine was antagonized by an intraperitoneal injection of atipamezole (0.1 mg/kg; Antisedan, 5 mg/mL, Orion Pharma).

2.5 | Imaging protocol

Images were acquired at 7 T on a Bruker Pharmascan (Bruker BioSpin, DE) in a double coil configuration. A 72-mm i.d. single channel transmission-only resonator was actively decoupled with a four-channel phased-array receive-only surface coil optimized for the rat brain.

After a scout image, T2w RARE images (TR = 5500 ms, TE = 76 ms, NEX = 8, MTX = 128 × 128 × 25, FOV = 35 × 35 × 25 mm, ACQtime = 5 min 20 s) were acquired for anatomical reference and to drive the coregistration step of the preprocessing. Multishot GRE-EPI pulse sequence was used for functional time series acquisition, with main parameters set as follows: TR = 500 ms, TE = 17 ms, NSHOTS = 4, NEX = 1, MTX = 96 × 96 × 10, FOV = 35 × 35 × 10 mm, NREP = 900, ACQtime = 30 min. Global shimming was refined by localized shimming with FASTMAP protocol.

Instead of the canonical single-shot EPI, here, we used a segmented EPI sequence as the latter provided a more robust and accurate

delineation of connectivity patterns along with a reduction in susceptibility artifacts.³³ These improvements were more prominent especially in deep brain nuclei and areas of the mesolimbic system, which are of interest for the current study. An additional set of high-resolution T2w RARE images (MTX = 256 × 256 × 25) was acquired for voxel-based morphometry (VBM) analysis after the resting state imaging session.

2.6 | Image analysis

Images were processed with MATLAB (The Mathworks, Inc.) and FSL (fmrib.ox.ac.uk/fsl). Raw data were converted to nifti format, and voxel size was scaled by a factor of 10 to be compliant with FSL algorithms. Preprocessing consisted of estimation and regression of motion confounds, slice timing correction, nonlinear high-pass, and gaussian low-pass filtering (0.01-0.1 Hz). Functional images were coregistered by 12 DOF affine transformations to structural T2w anatomical references and then resampled to a rat brain template in standard space.³⁴ After rigid body transformation, nonlinear warping to standard space was applied to further refine the normalization and minimize geometric distortions.

2.7 | Resting state networks identification

Independent component analysis with a high number of components ($n = 70$) was run at the subject level. ICA components were then hand-classified in a randomly sampled subset of subjects and labelled as noise or signal on the basis of spatial maps, frequency content, and features of time-course. This approach was effective in separating components related to subtle whole-head motion, CSF flow, ghosting, and between-shots motion artifacts. Spatial maps not related to anatomical structures, characterized by shifts towards high frequencies in the power spectrum or corrupted by clearly visible spikes, were classified as noise. Labels were used to train an automated classifier, and nonaggressive regression of noisy components was applied to the whole set of functional images. The performance of the classifier was assessed running a leave-one-out accuracy test using the previously defined set of hand-classified components. Denoised data were finally used to compute group level ICA with a reduced number of components ($d = 20$) in order to obtain a functional parcellation of the rat brain (<https://fsl.fmrib.ox.ac.uk/fsl/fslwiki/MELODIC>).

2.8 | Dual regression and connectivity of resting state components

Components obtained at the group level in the previous step were then used to feed a dual regression analysis.³⁵ In the first step, independent component maps were used as spatial regressors to obtain subject specific time series for each component. These time courses were then regressed against functional data to obtain subject specific version of the considered component. For each of these ICA-derived network, we considered the average value of the z-statistic image as

a metric to quantify within-component coherence at the subject level.³⁶ Time courses returned by the first step of dual regression were further used as input for network modelling (FSLNets), to assess the correlation between components and investigate how specific patterns of correlation could be altered either by ethanol exposure or pharmacological treatment. Artifactual components were excluded from the analysis by regressing out the corresponding time series. After this process, a total of seven functionally relevant components, involved in salience and reward processing, were considered for subsequent statistical analysis. Partial correlation between each pair of components was calculated for every subject and converted to z-statistic via standard Fisher's transform. These matrices were ultimately grouped to model between and within factors of a conventional two-way ANOVA analysis. An unpaired (between subjects) nonparametric test was run on correlation matrices with 5000 permutations to test for condition-specific differences in PD and alcohol-naïve rats. Two paired nonparametric tests were conducted within subjects for each group to assess differences in resting-state connectivity introduced by acute administration of the D3 antagonist SB-277011A. The interaction *Ethanol history condition* × *Treatment* was evaluated with a two-stage approach: first, paired (vehicle vs drug) differences of correlation matrices were computed for each group; the results were finally compared with an unpaired (PD vs ND) nonparametric test between conditions. The same statistical approach was used to test within-component functional connectivity changes induced by phenotype or treatment.

2.9 | Voxel-based morphometry

T2w RARE images, acquired at high resolution, were analysed to investigate voxelwise differences in local grey matter (GM) volume using a modified version of the FSL-VBM tool of FSL³⁷ to account for rat brain specific issues.³⁸ Briefly: an unbiased GM template was created by averaging group-balanced GM images ($n = 12$ ND and $n = 12$ PD rats). Individual GM volumes were registered to the

unbiased template using the FSL FNIRT algorithm³⁹ and then modulated (to correct for local deformations) by the Jacobian of the warp field, as reported in Ashburner and Friston.⁴⁰ The modulated GM images were then smoothed with an isotropic Gaussian kernel with a σ of 2.0 mm, and a nonparametric permutation test was applied.

3 | RESULTS

3.1 | ICA-based functional parcellation

Figure 1 shows the seven functionally relevant components identified by group ICA and known to be involved in AUD. Their spatial maps were used to extract the time-series and compute network functional correlation.

The components were named according to the underlying anatomy as follow: orbitofrontal-prelimbic cortex (OFC-PrL); accumbens (Acb); caudate putamen-anterior insula (CPu-AntIns); cingulate cortex (CgC); insula (Ins); retrosplenial Cortex (RsC); and ventral tegmental area (VTA). Because the ICA-based parcellation is a data-driven method that relies on statistical features of the voxel-wise signal, functional regions of interest may comprise multiple anatomically defined brain regions, as in the case of the OFC-PrL and CPu-AntIns components.

3.2 | Reduced functional connectivity within resting-state components

We considered the average value of the z-statistic image as a metric to quantify within-component coherence at the subject level. The between group statistical analysis revealed a widespread reduction of large-scale functional connectivity after CIE, particularly within the OFC-PrL ($*p_{FDR} < 0.05$), Acb ($*p_{FDR} < 0.01$), and CPu-AntIns ($*p_{FDR} < 0.05$) components (Figure 2A,B,C respectively). Noteworthy, a significant *Ethanol history condition* × *treatment* interaction ($^{\$}p_{FDR} < 0.05$), but not treatment, was observed for the Acb

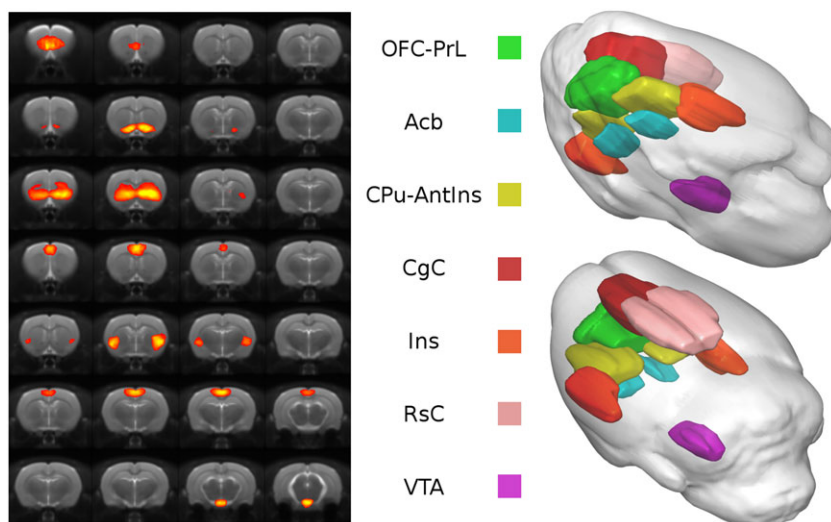


FIGURE 1 Functional parcellation of the rat brain. Spatial distribution (left side) and color-coded volume rendering (right side) of the seven meaningful components identified with ICA

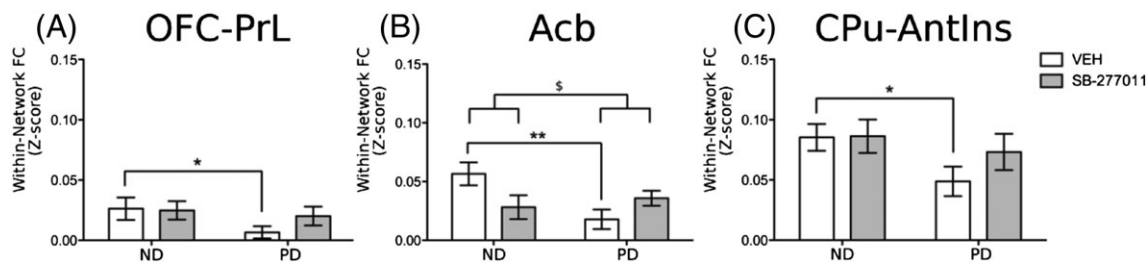


FIGURE 2 Within component connectivity. Significant alteration of within component connectivity is detected in A, OFC-PrL, B, Acb, and C, CPu-AntIns. Significant difference between ND and PD vehicle-treated groups: * $P < 0.05$ and ** $P < 0.01$. Significant *Ethanol history condition* \times *treatment* interaction § $P < 0.05$

component, suggesting that SB-277011-a modulated the connectivity of the Acb network differentially in the two groups of rats (PD vs ND). This effect may be the result of a dysregulation of dopamine receptor expression previously observed in PD rats.¹⁰

3.3 | A history of ethanol exposure altered the insular cortex connectivity

Unpaired nonparametric test run on vehicle-treated rats (ND vs PD) showed CIE-induced alteration of functional synchrony between different pairs of regions, reported in Figure 3A. Specifically, alcohol exposure decreased connectivity between the components CPu-AntIns and Ins (Figure 4A, * $p_{FDR} < 0.05$). Reduced correlation was also observed between the CgC and Ins (Figure 4B, * $p_{FDR} < 0.05$), which are commonly identified as constituents of the salience network.¹⁸ Additionally, decreased coupling was found between the retrosplenial cortex (RsC) and the nucleus accumbens (Acb) (* $p_{FDR} < 0.05$) (see Figure 3A). On the other hand, CIE strengthened functional coupling between areas of the mesolimbic system and regions of the salience network, specifically between VTA and CgC, VTA and CPu-AntIns, and between Acb and Ins (Figure 5A,B,C, respectively, * $p_{FDR} < 0.05$). Analysis of the effect of SB-277011-a revealed that the D3 antagonist does not significantly alter functional connectivity in ND rats (Figure 3B), whereas it shows a normalizing effect in the PD group (Figure 3C). In particular, acute administration of SB-277011-a in PD rats appears to restore the normal functional connectivity of the salience network: indeed, a significant increase in the strength of connectivity between the insular and cingulate cortex is observed in PD rats treated with the D3 antagonist compared with the vehicle group (CgC and Ins, Figure 4B, # $p_{FDR} < 0.05$).

Considering the contrasting results showing a decrease⁷ or an increase in functional coherence of the salience network in alcoholics,⁶ we performed additional, hypothesis-driven seed-based analysis with the agranular insula as anatomical seed to further corroborate our finding of a weaker correlation between the cingulate and the IC in PD rats, as well as of a restorative effect of SB-277011-a. This seed-based approach confirmed the results of our network correlation analysis, showing attenuation of CgC-Ins connectivity and normalization of the correlation strength after treatment with SB-277011-a in the PD group (see SI, Figure S3).

With regards to the increased connectivity observed after CIE between regions of the mesolimbic system and constituents of the salience network, again results showed an effect of SB-277011-a in attenuating the correlation between the VTA and cingulate cortex heightened by CIE in the PD group with a significant *Ethanol history condition* \times *Treatment* interaction (Figure 5A, # $p_{FDR} < 0.05$ and § $p_{FDR} < 0.05$).

Lastly, in PD rats, SB-277011-a also increased the correlation coefficient between the OFC and the Acb, an effect not observed in the ND group (Figure 3C).

3.4 | Voxel-based morphometry

Statistical analysis of structural imaging revealed no significant effect of CIE on GM volume between PD and ND vehicle-treated rats (TFCE corrected $P = 0.3$).

4 | DISCUSSION

Our results support the notion of widespread alterations in brain functional connectivity during early abstinence from alcohol dependence. The use of a well-established rodent model of AUD allows us to causally link alcohol to the observed change in functional connectivity during abstinence. Thereby, we can exclude potentially confounding factors such as nicotine use, other psychiatric comorbidities, or variable times of abstinence that typically hamper studies in clinical populations. Further, we demonstrate that such aberrant “abstinence network” states can be modified and at least partially reversed by pharmacotherapy, which suggests that fMRI-derived brain connectivity networks could be a potential biomarker for medication development.

Using a data-driven approach including unbiased independent component analysis, we found weaker internal coherence in addiction relevant components, specifically within the Acb-, OFC-PrL-, and CPu-AntIns components, of PD rats compared with alcohol-naive animals. This finding concurs with a study by Diaz-Parra and colleagues who showed by network-based statistic the disconnection of a sub-network comprising the hippocampus and other subcortical structures in PD rats compared with controls.⁴¹ Together with alteration of within-component connectivity, CIE induced changes in between-

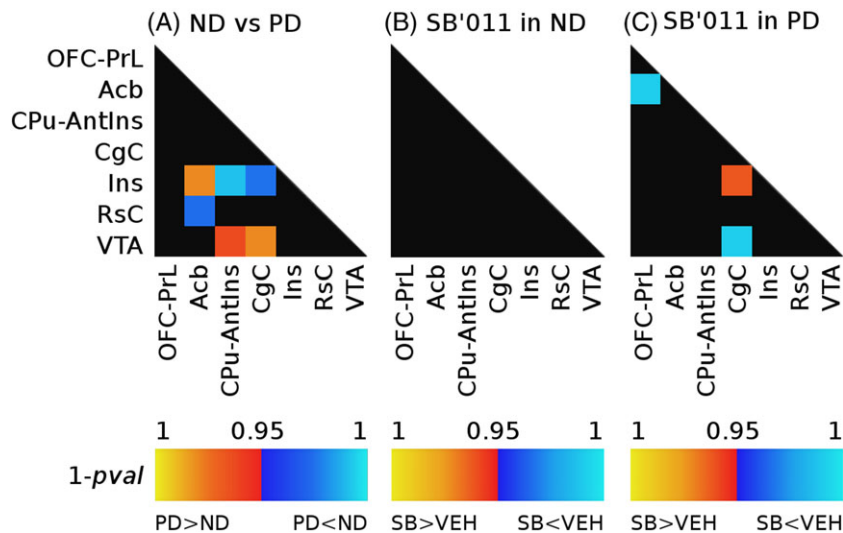


FIGURE 3 Modulation of between component connectivity after exposure to ethanol A, and acute administration of SB-277011-a in the nondependent B, and the postdependent group C. Warm colors indicate an increase in functional connectivity, whereas reduction of connectivity strength is shown in cool colors

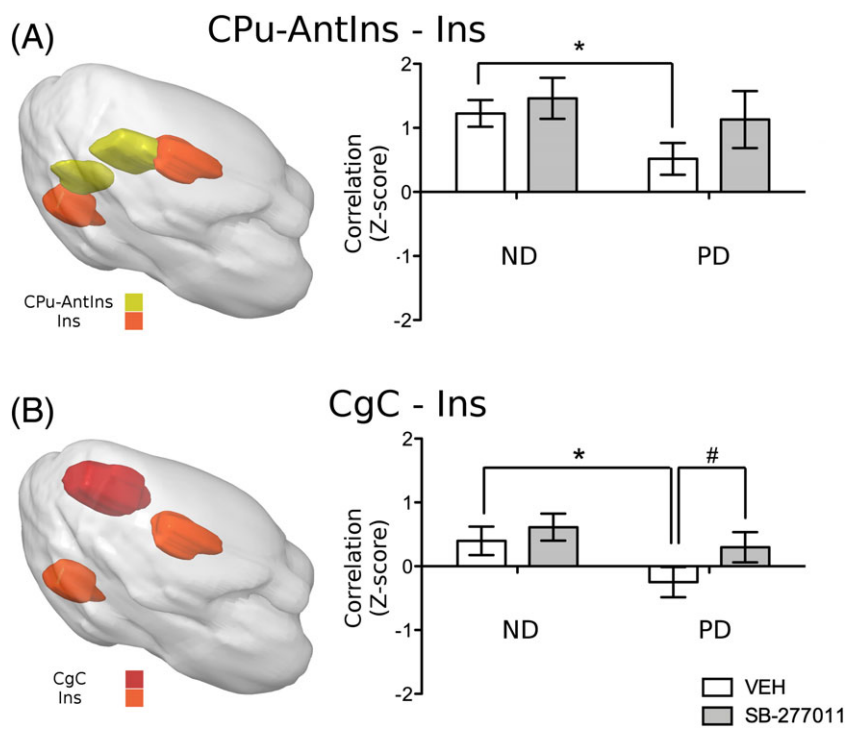


FIGURE 4 Altered functional connectivity of the insular cortex. A, 3D representation of the two components containing the insular cortex (CPu-AntIns and ins) and their correlation coefficient (expressed as mean \pm SEM). B, 3D spatial map of the salience network and mean \pm SEM of the correlation coefficients between its constituents (CgC and ins). Significant difference between ND and PD vehicle-treated groups: * $P < 0.05$. Significant difference between vehicle and SB-277011-a treated groups: # $P < 0.05$

components connectivity, especially involving the IC. Indeed, PD rats showed a decrease in functional coupling between subregions of the IC, namely the Ins and CPu-Ins components, and between the CgC and the Ins, elements of the salience network. On the other hand, a history of ethanol dependence strengthened the correlation between components of the salience network and mesolimbic areas.

Interestingly and in line with the restricted expression pattern of D3 receptors,^{19,20} SB-277011-a modulated Acb connectivity differentially in PD and ND rats. This effect could be due to the dysregulation of dopaminergic striatal systems observed in alcohol exposed rats during protracted withdrawal as well as in AUD patients.^{10,42} Furthermore, SB-277011-a partially restored aberrant connectivity in PD rats but had no significant effects in alcohol-naïve rats. Given that

we did not find structural differences between PD and ND rats according to VBM, the differential effect of SB-277011-a is likely due to differences in neural responsivity to the drug. Such an augmented response of neurochemical systems that are involved in the processing of alcohol's pharmacological effects has been found for a number of compounds, reviewed in Meinhardt and Sommer,⁹ and is an important feature of the PD model for medication development in AUD.

Our results in rodents showing aberrant functional connectivity of the IC are consistent with the implication of this area in drug addiction including alcoholism.^{15,16,43-45} The general notion emerging from these studies is that drug craving and cue-induced urges can be considered as complex interoceptive emotions that are processed in and

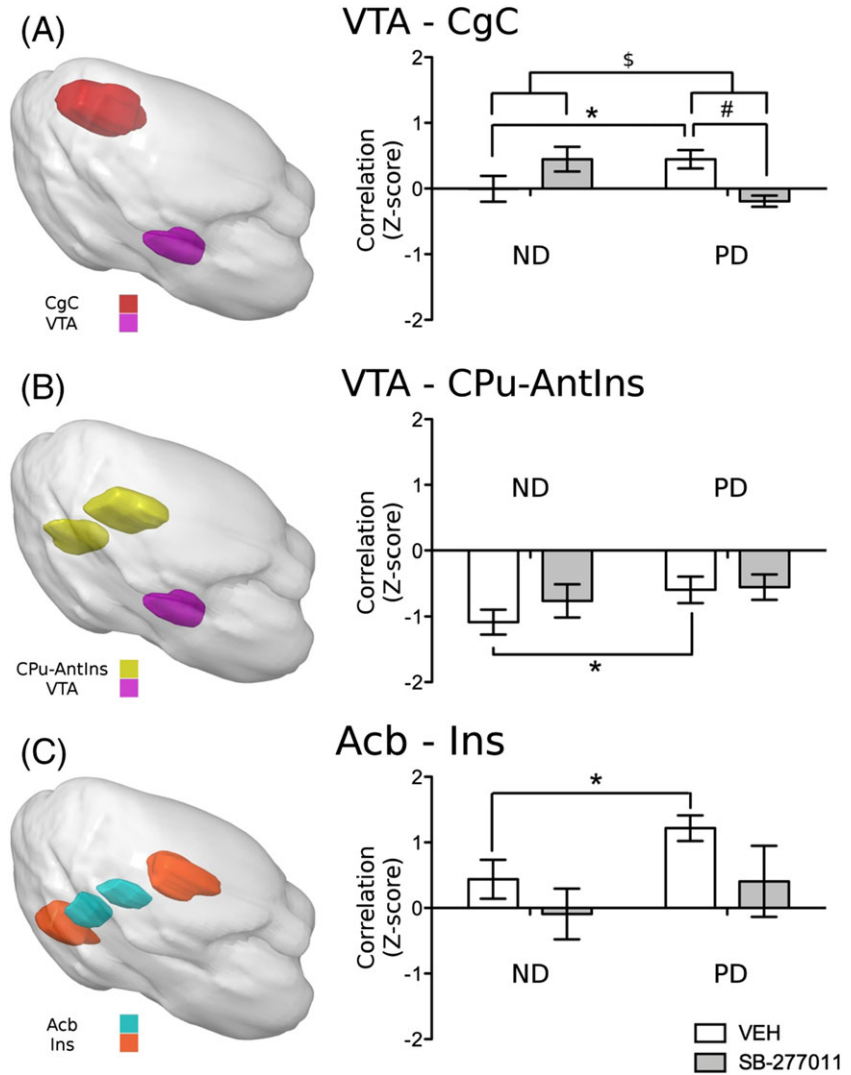


FIGURE 5 Altered functional correlation between the mesolimbic system and the salience network. Volumetric view and mean \pm SEM of the correlation coefficients between A, VTA and CgC; B, VTA and CPu-AntIns and C, the Acb and ins. Significant difference between ND and PD vehicle-treated groups: * $P < 0.05$. Significant difference between vehicle and SB-277011-a groups: # $P < 0.05$. Significant *Ethanol history condition* \times *treatment* interaction $^{\$}P < 0.05$

mapped to the IC, particularly in its anterior part, whereby the precise mechanisms of its involvement remain unclear. On one hand, several studies in humans and animals indicated diminished drug-seeking behaviors by insula lesions,^{43,45} an effect that was even more pronounced by combined damage of insula and putamen,⁴⁶ thus suggesting an abnormal connectivity of these two regions in addiction. Contrary to a general facilitatory role of the insula for drug seeking, reduced insula function was found in AUD subjects measured as a perfusion deficit in arterial spin-labelling MRI,¹⁶ and alcoholism is also associated with a loss of insula GM.¹⁵ Together, these findings indicate a highly complex involvement of insula in the control of addictive behaviors. Here, we found decreased resting state synchrony between the CPu-AntIns and Ins components as sequelae to chronic alcohol exposure in the absence of any morphometric changes to this brain region. The lack of overt structural damage to the insula in our preparation may not be surprising. In contrast to humans, where severe AUD takes decades to develop, the CIE procedure lasts only for about 2 months, which is apparently not sufficient to generate an advanced or end stage AUD condition. Nevertheless, our findings suggest insula involvement already early in the disease trajectory and that functional deficits may precede structural damage to this region.

The insula as a crucial node of the salience network is thought to be involved in directing attentional resources, accessing executive control processes, and driving behaviour.^{47,48} With regards to the AUD, decreased within-network connectivity of the salience network was found by resting-state fMRI,⁷ although another study reported the opposite effect.⁶ This inconsistency may be caused by differences in study populations. Importantly, a recent meta-analysis reported significantly decreased recruitment of the salience network during inhibitory control tasks in 30 reviewed studies investigating response inhibition in addicted individuals.⁴⁹ This finding parallels reports of increased measures of impulsivity in rodents with a history of chronic alcohol exposure.^{9,50,51} Besides decreased connectivity within the salience network, we also observed increased coupling between constituents of the salience and the reward system in PD rats. Similarly, human drug users showed tightened coupling between the salience and the reward networks.⁴⁹ This finding was interpreted as a neural substrate of the increased salience given to the drug or drug-associated cues after chronic consumption as predicted by common theories of addiction.⁵²⁻⁵⁴ The aberrant connectivity we observed between the Acb-Ins in PD rats is consistent with this interpretation. Altered connectivity between these two regions is also

suggested by Seif and colleagues, who demonstrated a critical role for the insula-to-accumbens inputs in mediating aversion-resistant alcohol intake in rodents.⁵⁵ Furthermore, we found increased connectivity between VTA and CgC in alcohol exposed rats. CgC provides top-down control to the VTA thereby modulating the motivation to pursue a reward.⁵⁶ This pathway is also implicated in the inhibition of cocaine seeking in rats.⁵⁷

Notably, treatment with SB-277011-a restored the aberrant connectivity within the salience network components and between salience and reward networks in PD rats. It seems plausible to hypothesize that these fMRI signatures could be related to the compound's efficacy in cue-induced, stress-induced, and drug-induced reinstatement of drug seeking including in rodent models of AUD.^{21,24,58-60} With regard to PD rats, at the time of the fMRI investigation, ie, 3 to 4 weeks of abstinence, they are in a hyperdopaminergic state.¹⁰ This dysregulation of the mesolimbic dopamine system may drive the increased functional connectivity between VTA and CgC components observed here and reversed by SB-277011-a.

The present study was performed under anaesthesia using the alpha-2-adrenergic agonist medetomidine. This method was recently introduced for fMRI studies in rodents^{32,38} particularly because it does not require catheterization and assisted breathing, thus allowing for longitudinal experimental designs. Importantly, low doses of medetomidine, as we used here, produce sedation, rather than full anaesthesia, and thus may preserve, at least to some extent, the integrity of functional connectivity networks, as reported in previous studies.^{3,61} Furthermore, measurement of functional connectivity in awake animals may be affected by motion and stress.

In conclusion, by means of a hypothesis free analysis, our study showed that a history of alcohol dependence alters brain connectivity at rest with a prominent involvement of networks comprising the IC. Specifically, we observed weaker connectivity between insular and cingulate cortex in the salience network, and stronger connectivity between the insula and constituents of the mesolimbic reward system. Importantly, acute administration of the D3 selective antagonist, SB-277011-a, a compound shown to decrease drug consumption and relapse in animals models of abuse, including alcohol, normalized the aberrant connectivity induced by CIE to ethanol. This study suggests that modulation of specific nodes in the networks involved in addiction may normalize the overall brain connectivity, thus shedding new light on the putative underlying mechanism of action.

ACKNOWLEDGEMENTS

This project has received funding from the European Union's Horizon 2020 research and innovation program under grant agreement no. 668863 (SyBil-AA).

DISCLOSURES

The authors declare no conflict of interest.

AUTHOR CONTRIBUTION

G.S., A.B., and W.H.S. were responsible for the study concept and design. G.S. and S.T. performed the experiment, analysed the data, and wrote the manuscript. S.P. provided the PD rat model and contributed to data collection. A.B. and W.S. provided critical revision of the manuscript for important intellectual content. All authors critically reviewed the content and approved the final version for publication.

ORCID

Giulia Scuppa  <https://orcid.org/0000-0002-7641-1493>

REFERENCES

1. Biswal B, Yetkin FZ, Haughton VM, Hyde JS. Functional connectivity in the motor cortex of resting human brain using echo-planar MRI. *Magn Reson Med*. 1995;34(4):537-541.
2. Ogawa S, Lee TM, Kay AR, Tank DW. Brain magnetic resonance imaging with contrast dependent on blood oxygenation. *Proc Natl Acad Sci U S A*. 1990;87(24):9868-9872.
3. Lu H, Zou Q, Gu H, Raichle ME, Stein EA, Yang Y. Rat brains also have a default mode network. *Proc Natl Acad Sci*. 2012;109(10):3979-3984.
4. Shen HH. Core concept: resting-state connectivity. *Proc Natl Acad Sci U S A*. 2015;112(46):14115-14116.
5. Jansen JM, van Wingen G, van den Brink W, Goudriaan AE. Resting state connectivity in alcohol dependent patients and the effect of repetitive transcranial magnetic stimulation. *Eur Neuropsychopharmacol*. 2015;25(12):2230-2239.
6. Zhu X, Cortes CR, Mathur K, Tomasi D, Momenan R. Model-free functional connectivity and impulsivity correlates of alcohol dependence: a resting-state study. *Addict Biol*. 2017;22(1):206-217.
7. Müller-Oehring EM, Jung Y-C, Pfefferbaum A, Sullivan EV, Schulte T. The resting brain of alcoholics. *Cereb Cortex*. 2015;25(11):4155-4168.
8. Heilig M, Koob GF. A key role for corticotropin-releasing factor in alcohol dependence. *Trends Neurosci*. 2007;30(8):399-406.
9. Meinhardt MW, Sommer WH. Postdependent state in rats as a model for medication development in alcoholism. *Addict Biol*. 2015;20(1):1-21.
10. Hirth N, Meinhardt MW, Noori HR, et al. Convergent evidence from alcohol-dependent humans and rats for a hyperdopaminergic state in protracted abstinence. *Proc Natl Acad Sci*. 2016;113(11):3024-3029.
11. Sommer WH, Rimondini R, Hansson AC, et al. Upregulation of voluntary alcohol intake, behavioral sensitivity to stress, and amygdala Crhr1 expression following a history of dependence. *Biol Psychiatry*. 2008;63(2):139-145.
12. Meinhardt MW, Hansson AC, Perreau-Lenz S, et al. Rescue of Infralimbic mGluR2 deficit restores control over drug-seeking behavior in alcohol dependence. *J Neurosci*. 2013;33(7):2794-2806.
13. Egli M. Advancing pharmacotherapy development from preclinical animal studies. In: Grant K, Lovinger D, eds. *The Neuropharmacology of Alcohol. Handbook of Experimental Pharmacology*. Cham: Springer; 2018:248.
14. Broadwater MA, Lee S-H, Yu Y, et al. Adolescent alcohol exposure decreases frontostriatal resting-state functional connectivity in adulthood. *Addict Biol*. 2018;23(2):810-823.
15. Senatorov VV, Damadzic R, Mann CL, et al. Reduced anterior insula, enlarged amygdala in alcoholism and associated depleted von Economo neurons. *Brain*. 2015;138(1):69-79.

16. Sullivan EV, Müller-Oehring E, Pitel A-L, et al. A selective insular perfusion deficit contributes to compromised salience network connectivity in recovering alcoholic men. *Biol Psychiatry*. 2013;74(7):547-555.
17. Menon V, Uddin LQ. Saliency, switching, attention and control: a network model of insula function. *Brain Struct Funct*. 2010;214(5-6):655-667.
18. Seeley WW, Menon V, Schatzberg AF, et al. Dissociable intrinsic connectivity networks for salience processing and executive control. *J Neurosci*. 2007;27(9):2349-2356.
19. Bouthenet M-L, Souil E, Martres M-P, Sokoloff P, Giros B, Schwartz J-C. Localization of dopamine D3 receptor mRNA in the rat brain using in situ hybridization histochemistry: comparison with dopamine D2 receptor mRNA. *Brain Res*. 1991;564(2):203-219.
20. Sokoloff P, Giros B, Martres M-P, Bouthenet M-L, Schwartz J-C. Molecular cloning and characterization of a novel dopamine receptor (D3) as a target for neuroleptics. *Nature*. 1990;347(6289):146-151.
21. Heidbreder CA, Andreoli M, Marcon C, Hutcheson DM, Gardner EL, Ashby CR. Evidence for the role of dopamine D3 receptors in oral operant alcohol self-administration and reinstatement of alcohol-seeking behavior in mice. *Addict Biol*. 2007;12(1):35-50.
22. Rice OV, Schonhar CA, Gaál J, Gardner EL, Ashby CR. The selective dopamine D₃ receptor antagonist SB-277011-a significantly decreases binge-like consumption of ethanol in C57BL/J6 mice. *Synapse*. 2015;69(6):295-298.
23. Thanos P, Katana J, Ashbyjr C, et al. The selective dopamine D3 receptor antagonist SB-277011-a attenuates ethanol consumption in ethanol preferring (P) and non-preferring (NP) rats. *Pharmacol Biochem Behav*. 2005;81(1):190-197.
24. Vengeliene V, Leonardi-Essmann F, Perreau-Lenz S, et al. The dopamine D3 receptor plays an essential role in alcohol-seeking and relapse. *FASEB J*. 2006;20(13):2223-2233.
25. Heilig M, Barbier E, Johnstone AL, et al. Reprogramming of mPFC transcriptome and function in alcohol dependence. *Genes Brain Behav*. 2017;16(1):86-100.
26. Rimondini R, Arlinde C, Sommer W, Heilig M. Long-lasting increase in voluntary ethanol consumption and transcriptional regulation in the rat brain after intermittent exposure to alcohol. *FASEB J*. 2002;16(1):27-35.
27. Schwarz A, Gozzi A, Reese T, et al. Selective dopamine D3 receptor antagonist SB-277011-a potentiates pHMRI response to acute amphetamine challenge in the rat brain. *Synapse*. 2004;54(1):1-10.
28. Schwarz AJ, Gozzi A, Reese T, Heidbreder CA, Bifone A. Pharmacological modulation of functional connectivity: the correlation structure underlying the pHMRI response to d-amphetamine modified by selective dopamine D3 receptor antagonist SB277011A. *Magn Reson Imaging*. 2007;25(6):811-820.
29. Rice OV, Gardner EL, Heidbreder CA, Ashby CR Jr. The acute administration of the selective dopamine D(3) receptor antagonist SB-277011A reverses conditioned place aversion produced by naloxone precipitated withdrawal from acute morphine administration in rats. *Synapse*. 2012;66(1):85-87.
30. Gozzi A, Schwarz A, Crestan V, Bifone A. Drug-anaesthetic interaction in pHMRI: the case of the psychotomimetic agent phencyclidine. *Magn Reson Imaging*. 2008;26(7):999-1006.
31. D'Souza DV, Jonckers E, Bruns A, et al. Preserved modular network organization in the sedated rat brain. *PLoS ONE*. 2014;9(9):e106156. <https://doi.org/10.1371/journal.pone.0106156>
32. Pawela CP, Biswal BB, Hudetz AG, et al. A protocol for use of medetomidine anesthesia in rats for extended studies using task-induced BOLD contrast and resting-state functional connectivity. *Neuroimage*. 2009;46(4):1137-1147.
33. Tambalo S, Scuppa G, Bifone A. Segmented echo planar imaging improves detection of subcortical functional connectivity networks in the rat brain. *Sci Rep*. 2019;9(1):1397.
34. Schwarz AJ, Danckaert A, Reese T, et al. A stereotaxic MRI template set for the rat brain with tissue class distribution maps and co-registered anatomical atlas: application to pharmacological MRI. *Neuroimage*. 2006;32(2):538-550.
35. Nickerson LD, Smith SM, Öngür D, Beckmann CF. Using dual regression to investigate network shape and amplitude in functional connectivity analyses. *Front Neurosci*. 2017;11:115.
36. Tommasin S, Mascali D, Moraschi M, et al. Scale-invariant rearrangement of resting state networks in the human brain under sustained stimulation. *Neuroimage*. 2018;179:570-581.
37. Smith SM, Jenkinson M, Woolrich MW, et al. Advances in functional and structural MR image analysis and implementation as FSL. *Neuroimage*. 2004;23:5208-5219.
38. Tambalo S, Peruzzotti-Jametti L, Rigolio R, et al. Functional magnetic resonance imaging of rats with experimental autoimmune encephalomyelitis reveals brain cortex remodeling. *J Neurosci*. 2015;35(27):10088-10100.
39. Schnabel JA, Tanner C, Castellano-Smith AD, et al. Validation of non-rigid image registration using finite-element methods: application to breast MR images. *IEEE Trans Med Imaging*. 2003;22(2):238-247.
40. Ashburner J, Friston KJ. Voxel-based morphometry—the methods. *Neuroimage*. 2000;11(6):805-821.
41. Diaz-Parra A, Perez-Ramirez U, Pacheco-Torres J, et al. Evaluating network brain connectivity in alcohol postdependent state using network-based statistic. In: 2017 39th Annual International Conference of the IEEE Engineering in Medicine and Biology Society (EMBC) IEEE; 2017:533-536.
42. Hansson AC, Gründer G, Hirth N, Noori HR, Spanagel R, Sommer WH. Dopamine and opioid systems adaptation in alcoholism revisited: convergent evidence from positron emission tomography and postmortem studies. *Neurosci Biobehav Rev*. 2018. <https://doi.org/10.1016/j.neubiorev.2018.09.010>
43. Contreras M, Ceric F, Torrealba F. Inactivation of the interoceptive insula disrupts drug craving and malaise induced by lithium. *Science*. 2007;318(5850):655-658.
44. Heilig M, Epstein DH, Nader MA, Shaham Y. Time to connect: bringing social context into addiction neuroscience. *Nat Rev Neurosci*. 2016;17(9):592-599.
45. Naqvi NH, Rudrauf D, Damasio H, Bechara A. Damage to the insula disrupts addiction to cigarette smoking. *Science*. 2007;315(5811):531-534.
46. Gaznick N, Tranel D, McNutt A, Bechara A. Basal ganglia plus insula damage yields stronger disruption of smoking addiction than basal ganglia damage alone. *Nicotine Tob Res*. 2014;16(4):445-453.
47. Corbetta M, Patel G, Shulman GL. The reorienting system of the human brain: from environment to theory of mind. *Neuron*. 2008;58(3):306-324.
48. Naqvi NH, Bechara A. The hidden island of addiction: the insula. *Trends Neurosci*. 2009;32(1):56-67.
49. Zilverstand A, Huang AS, Alia-Klein N, Goldstein RZ. Neuroimaging impaired response inhibition and salience attribution in human drug addiction: a systematic review. *Neuron*. 2018;98(5):886-903.
50. Irimia C, Tuong RN, Quach T, Parsons LH. Impaired response inhibition in the rat 5 choice continuous performance task during protracted

- abstinence from chronic alcohol consumption. *PLoS ONE*. 2014;9(10):e109948. <https://doi.org/10.1371/journal.pone.0109948>
51. Radke AK, Jury NJ, Kocharian A, et al. Chronic EtOH effects on putative measures of compulsive behavior in mice. *Addict Biol*. 2017;22(2):423-434.
52. Everitt BJ, Robbins TW. Drug addiction: updating actions to habits to compulsions ten years on. *Annu Rev Psychol*. 2016;67(1):23-50.
53. Goldstein RZ, Volkow ND. Drug addiction and its underlying neurobiological basis: neuroimaging evidence for the involvement of the frontal cortex. *Am J Psychiatry*. 2002;159(10):1642-1652.
54. Koob GF, Volkow ND. Neurobiology of addiction: a neurocircuitry analysis. *Lancet Psychiatry*. 2016;3(8):760-773.
55. Seif T, Chang S-J, Simms JA, et al. Cortical activation of accumbens hyperpolarization-active NMDARs mediates aversion-resistant alcohol intake. *Nat Neurosci*. 2013;16(8):1094-1100.
56. Elston TW, Bilkey DK. Anterior cingulate cortex modulation of the ventral tegmental area in an effort task. *Cell Rep*. 2017;19(11):2220-2230.
57. Navailles S, Guillem K, Vouillac-Mendoza C, Ahmed SH. Coordinated recruitment of cortical-subcortical circuits and ascending dopamine and serotonin neurons during inhibitory control of cocaine seeking in rats. *Cereb Cortex*. 2015;25(9):3167-3181.
58. Heidbreder C. Rationale in support of the use of selective dopamine D3 receptor antagonists for the pharmacotherapeutic management of substance use disorders. *Naunyn Schmiedebergs Arch Pharmacol*. 2013;386(2):167-176.
59. Khaled MATM, Pushparaj A, Di Ciano P, Diaz J, Le Foll B. Dopamine D3 receptors in the basolateral amygdala and the lateral habenula modulate cue-induced reinstatement of nicotine seeking. *Neuropsychopharmacology*. 2014;39(13):3049-3058.
60. Sabioni P, Di Ciano P, Le Foll B. Effect of a D3 receptor antagonist on context-induced reinstatement of nicotine seeking. *Prog Neuro-Psychopharmacol Biol Psychiatry*. 2016;64:149-154.
61. Bajic D, Craig MM, Mongerson CRL, Borsook D, Becerra L. Identifying rodent resting-state brain networks with independent component analysis. *Front Neurosci*. 2017;11:685.

SUPPORTING INFORMATION

Additional supporting information may be found online in the Supporting Information section at the end of the article.

How to cite this article: Scuppa G, Tambalo S, Pfarr S, Sommer WH, Bifone A. Aberrant insular cortex connectivity in abstinent alcohol-dependent rats is reversed by dopamine D3 receptor blockade. *Addiction Biology*. 2020;25:e12744. <https://doi.org/10.1111/adb.12744>